**Detailed description of TLM**

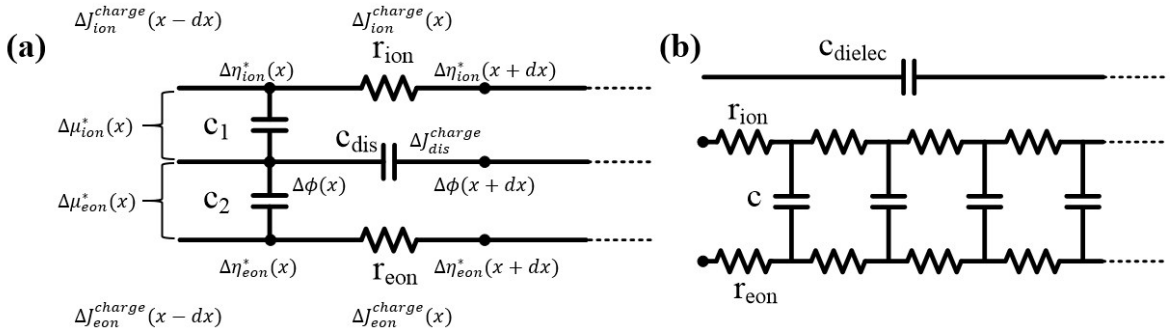


Fig. S1. (a) Differential element of the equivalent circuit representing a system in which electrons and ions are mobile. [1] (b) Equivalent circuit obeying local charge neutrality.

In solid-state electrochemistry, when a mixed conducting material is subject to an electrical potential, stoichiometric gradients are built up internally. Also, when such mixed conductor is subject across a chemical gradient, ambipolar flux develops. All these conditions and resulting effects could be mathematically expressed using the well-known transport equation (1), continuity equations (2) and Poisson's equations (3).

$$J_i^{mass}(x,t) = -D_i\frac{\partial c_i(x,t)}{\partial x} - \frac{\sigma_i(x,t)\partial\phi(x,t)}{z_i e\ \ \partial x} \quad (1)$$

$$\frac{\partial J_i^{mass}(x,t)}{\partial x} + \frac{\partial c_i(x,t)}{\partial t} = 0 \quad (2)$$

$$-\varepsilon_r(x,t)\varepsilon_0\frac{\partial^2\phi(x,t)}{\partial x^2} = \sum_i e z_i c_i(x,t) \quad (3)$$

As in the literature of J. Jamnik and J. Maier [2], MIEC's transmission line model includes an electric rail, an ion rail and a displacement rail (Fig.S1a; in this figure, fluxes, $\Delta J_i^{charge}$ and $\Delta J_{dis}^{charge}$, are caused by small perturbation of electrochemical potential$\{\Delta\eta_i = \Delta\mu_i + z_i e\Delta\phi\}$ and electric potential$\{\Delta\phi\}$, respectively). The species of the electron rail and the ion rail are affected by the electrochemical potential gradient of each spices, and the displacement line is affected by the external electric potential. The voltage difference between the displacement rail and the electron rail is due to the electron's chemical potential gradient. Likewise, the voltage difference with the ion rail is due to the chemical potential gradient of the ion. If the electric neutral condition is satisfied, the flux flowing from the electromagnetic rail to the displacement will cancel the flux from the ion rail to the displacement rail. Therefore, displacement rails can be separated and expressed as shown in the Fig.S1b, and differential equations can be derived using circuit law (Ohm's law and Kirchhoff's 2nd laws).

After that, an equation such as Eq. 2 is obtained by using the boundary conditions suitable for the cell configuration. For example, the Bisquert model [3] takes into consideration a liquid electrolyte interfaced to an electron conducting porous electrode. Herein, only ions pass through one terminal, while only electrons pass through the other ($\Delta J_{ion}^{charge}(L) = 0\ and\ \Delta J_{eon}^{charge}(0) = 0$). Because of this asymmetric characteristic of both ends, the boundary condition used by Bisquert was used in SOFC electrodes as shown in Figure 2b. On the other hand, in Lai's paper [1], they measured 10% gadolinium doped ceria (GDC10) sandwiched by Pt electrodes, which leads to a symmetric cell configuration. So, it is possible to use same boundary conditions at both terminals because both electrode/MIEC interface is same. Although both cases have different boundary conditions, the mathematical models for the charge fluxes in TLM is governed by the eq. (1) ~ (3).

In general, the material used in fuel cell electrodes has an electron conductivity much higher than that of ion conductivity, so the resistance of the electron rail can be neglected. ($r_{eon}$=0) In the case of densely structured MIEC, $r_{ion}$ is entirely the resistance to the movement of ions in the bulk. However, the electrode of the actual fuel cell uses a porous electrode. Then, not only the bulk ions but also the ions adsorbed on the surface of the electrode move under the same force. In addition, since the porous electrode has a much larger surface area, $r_p$ and c connected in parallel with each rail also differ from the dense electrode. $R_p$, which means the resistance of the reaction at the surface, will become smaller due to the large surface area, and c as the chemical capacitance may be affected by the adsorption capacitance due to the adsorbed ions.

**Half-cell measurement**

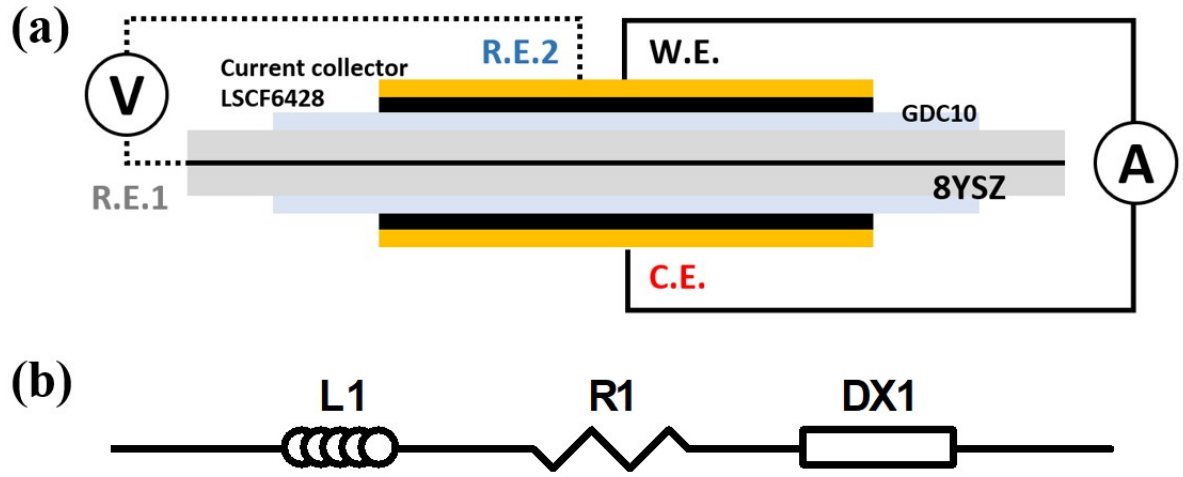


Fig. S2. (a) Schematic representation of the half-cell configuration. In case of infiltrated cell, both electrodes were infiltrated by the solution. (b) Equivalent circuit model used in fitting of half-cell. L1 represents a system inductance, R1 an ohmic resistance and DX1 polarization resistance of the electrode.

Half-cell measurement is an easier measurement method. Full-cell fitting may be more difficult than half-cell because each electrode reaction overlaps at similar frequencies. However, it must also be considered that symmetrical cell measurements are kind of simulated conditions which doesn't reflect the actual fuel cell operation. In this section, the fitting results of two half-cells (original and infiltrated) were compared to those of full-cells. In Fig.S2a, schematic half-cell measurement system can be seen. Temperature was varied in the range of 800~600℃ and $pO_2$ was set to 0.21atm. The infiltrated cell was fabricated by adding the solution on both electrodes. EIS were measured in frequency range of $10^6$ ~ $10^{-1}$ Hz as shown in Fig.S3a and b. $Z_{re}$ values were subtracted by each high frequency intercept for easy comparison.

Fig.3c and d show the transmission line parameters ($R_s$, $R_p$ and $C_p$) fit by the equivalent circuit model shown in Fig.S2b. It can be seen that the value of the infiltration cell has more difference than that of the original cell. In particular, since $R_s$ overlaps with the gas diffusion resistance of the anode, this effect seems to show a larger error. It was confirmed that the difference in $C_p$ value of the infiltration cell was also larger. However, except for $R_s$, the differences were within one order of magnitude.

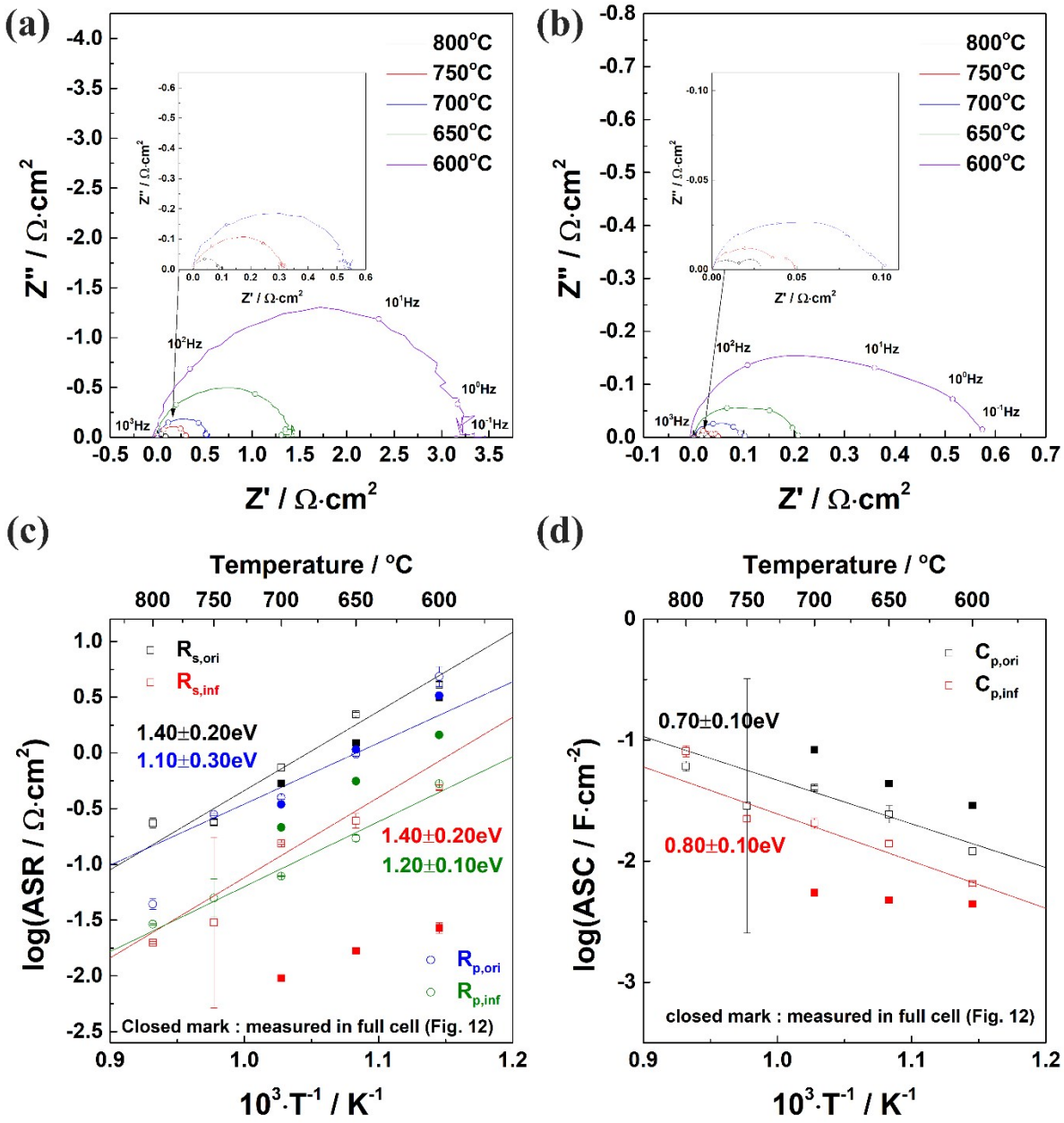


Fig. S3. (a, b) Nyquist plot of impedance spectra of original and infiltrated half-cell. (c, d) TLM parameters comparison between the original and infiltrated half-cell as a function of temperature (800~600 ℃). $pO_2$ was set to 0.21atm. Fit results were tabulated in Table S3 and S4.

**Reference**

[1] W. Lai and S. Haile, J. Am. Ceram. Soc., 88 (2005), 2979-2997

[2] J. Jamnik and J. Maier, Journal of The Electrochemical Society, 1999, 146, 4183.

[3] J. Bisquert, Phys. Chem. Chem. Phys., 2000, 2, 4185–4192.